ACS Catalysis

pubs.acs.org/acscatalysis

Research Article

Cofactor Binding Dynamics Influence the Catalytic Activity and Selectivity of an Artificial Metalloenzyme

Lara Villarino,* Shreyans Chordia, Lur Alonso-Cotchico, Eswar Reddem, Zhi Zhou, Andy Mark W. H. Thunnissen, Jean-Didier Maréchal, and Gerard Roelfes*

Cite This: *ACS Catal.* 2020, 10, 11783−11790

Read Online

ACCESS | Metrics & More | Article Recommendations | Supporting Information

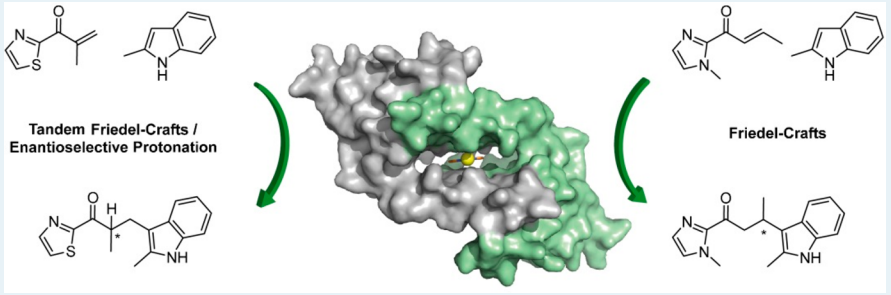

ABSTRACT: We present an artificial metalloenzyme based on the transcriptional regulator LmrR that exhibits dynamics involving the positioning of its abiological metal cofactor. The position of the cofactor, in turn, was found to be related to the preferred catalytic reactivity, which is either the enantioselective Friedel−Crafts alkylation of indoles with β-substituted enones or the tandem Friedel−Crafts alkylation/enantioselective protonation of indoles with α-substituted enones. The artificial metalloenzyme could be specialized for one of these catalytic reactions introducing a single mutation in the protein. The relation between cofactor dynamics and activity and selectivity in catalysis has not been described for natural enzymes and, to date, appears to be particular for artificial metalloenzymes.

KEYWORDS: *artificial metalloenzymes, biocatalysis, structural dynamics, enzyme design, copper*

INTRODUCTION

Enzymes are remarkable catalysts, capable of catalyzing chemical transformations with high rates and selectivities. A popular approach to achieve enzymatic catalysis of reactions that have no equivalent in nature involves the creation of artificial metalloenzymes, which are rationally designed hybrids of proteins with abiological catalytically active metal cofactors.[1−7] In this approach, the basal catalytic activity is supplied by the metal complex, whereas the second coordination sphere interactions provided by the protein scaffold are envisioned to contribute to rate acceleration and (enantio-)selectivity. Since the protein scaffolds used have not naturally evolved for the reaction of interest, usually the active site structure is far from optimal.

One key to the ability of enzymes to accelerate reactions is their ability to provide structural complementarity of the active site to the activated complex of the catalyzed reaction by taking advantage of structural dynamics.[8] The dynamics of the protein involve conformational changes, e.g., domain rearrangement, loop motions, partial folding/unfolding, etc., crucial to reach the optimal structure of the active site. Those flexible regions are also frequently involved in the emergence of alternative active site structures and relate to promiscuous catalytic activities. Thus, they are important targets for mutagenesis in the natural- or directed evolution of enzymes, including artificial metalloenzymes, to improve the activity.[9−18]

A special subset of structural dynamics involves the dynamics in binding of a metal cofactor, that is, the interchange of cofactor position between multiple cofactor binding sites. This is uncommon in natural enzymes as these usually employ highly evolved cofactor binding sites. However, artificial metalloenzymes are more rudimentary and have not evolved for binding abiological cofactors. Hence, it is possible that the cofactor can bind at multiple sites, that all contribute to the overall catalysis results depending on their relative abundance and their activity in catalysis. For example, in artificial metalloenzymes created by dative binding of rhodium complexes to apo carbonic anhydrase, the rhodium centers were found to bind at multiple sites in the protein in addition

Received: April 9, 2020
Revised: September 11, 2020
Published: September 18, 2020

https://dx.doi.org/10.1021/acscatal.0c01619
ACS Catal. 2020, 10, 11783−11790

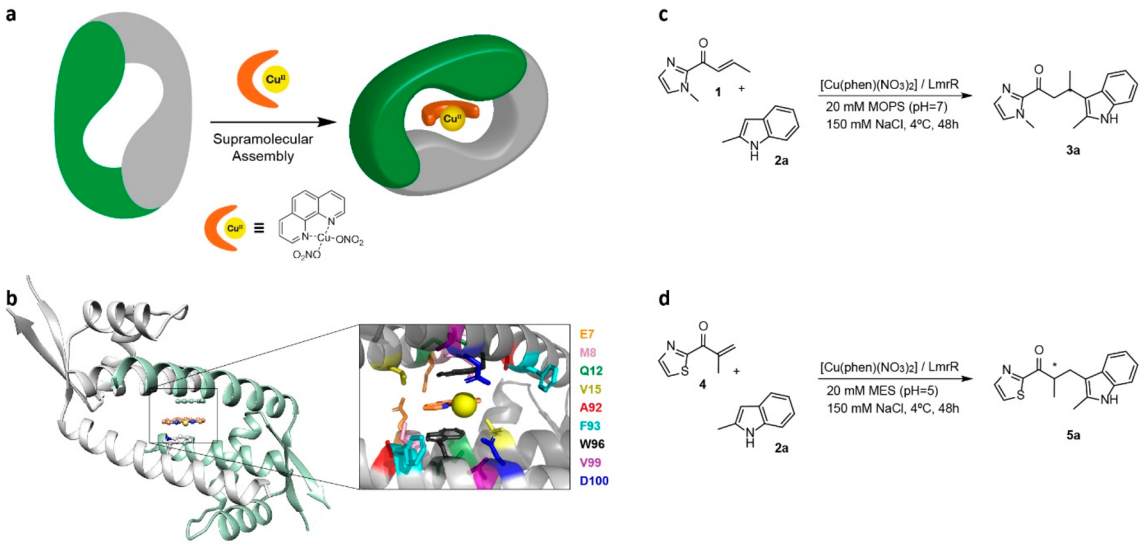

Figure 1. (a) Schematic representation of the self-assembly of the artificial metalloenzyme. (b) Crystal structure of the LmrR/Cu(II)-phen artificial metalloenzyme (PDB: 6R1L). Considerable disorder is observed in the binding mode of Cu-phen, as evidenced by its relatively weakly associated electron density and high atomic B-factors. Disordered ligand binding is a general observation in crystal structures of LmrR and may be an inherent property of this protein. Unfortunately, the weak electron density around the copper, and its special position in the crystal on a crystallographic dyad, prohibited an unambiguous identification of its coordination geometry and ligands other than phenantroline. Close up view of the hydrophobic pore of the LmrR. Residues used in the mutagenesis study are highlighted as sticks (color code as indicated). (c) catalyzed FC reaction (d) catalyzed FC/EP reaction.

to the primary metal binding site.[19−21] Moreover, cofactor binding dynamics has been shown to be of key importance in the DNA equivalent of artificial metalloenzymes.[22] We have reported in supramolecular DNA-based catalysis that metal complexes such as copper bipyridine bind reversibly at many different locations in the DNA, resulting in many actives sites with differently structured microenvironments in which catalysis occurs with different activity and selectivity.[23] As a result, the overall result of catalysis is the weighted average of the contribution of all these individual sites.[24]

Here, we report that dynamics in the binding position of an abiological metal cofactor in an artificial metalloenzyme leads to alternative active site structures in the same protein. We also show how the activity and enantioselectivity of this artificial metalloenzyme in two related reactions is dependent on the position of the metal cofactor in the protein scaffold. Finally, by a single mutation the artificial metalloenzyme can be specialized toward either of these two catalytic reactions.

RESULTS AND DISCUSSION

ARM Assembly and Structure. The design of the artificial metalloenzyme is based on the transcription factor Lactococcal multidrug resistance Regulator (LmrR), which is a homodimeric protein with a size of 13.5 kDa per monomer that contains an unusually large hydrophobic pore at the dimer interface.[25] This hydrophobic pore serves as a promiscuous binding pocket where planar aromatic molecules bind, as shown in X-ray and NMR structures of LmrR with various planar drugs bound.[25−27] Two tryptophan residues, one from each subunit, i.e., W96 and W96′, play a key role in binding by sandwiching the guest molecule via π-stacking interactions. Previously, we have shown that this arrangement is attractive for the supramolecular self-assembly of a novel artificial metalloenzyme, by combining LmrR with a Cu(II) complex with a planar aromatic ligand, like 1,10-phenanthroline (phen; Figure 1a).[28,29] LmrR showed a moderately strong affinity for Cu(II)-phen, with a dissociation constant (K_d) of 2.6 ± 2 μM. The importance of the central tryptophans for binding Cu(II)-phen is illustrated by the fact that in case of the mutant LmrR_W96A, the K_d was 1 order of magnitude lower, i.e., 45 μM.

The binding of Cu(II)-phen to LmrR was confirmed by X-ray crystallography, which showed the phenanthroline ligand of the complex sandwiched between W96 and W96′, with the indole rings somewhat tilted with respect to each other and the Cu(II) complex (Figure 1b). The Cu(II) ion is facing the front entrance of the pore. Two carboxylate side chains, from D100 and D100′ are oriented toward the Cu(II) ion at a distance of ∼5 Å and may interact with bound ligands, e.g., water, at the remaining coordination sites at the copper, albeit that these could not be identified with certainty. Protein residues other than W96 and D100 that surround the copper within a distance of 8 Å are predominantly hydrophobic, i.e., V15, A92, S97, V99, and I103 (and their equivalents from the dimer mate).

Catalysis. In this study, we focused on the application of the artificial enzymes in two catalytic reactions. First, the previously reported enantioselective vinylogous Friedel−Crafts alkylation of indoles with α, β unsaturated 2-acyl-imidazoles (FC reaction), which gives rise to excellent enantioselectivities, to up to 92% ee when catalyzed by LmrR/Cu(II)-phen (Figure 1c).[28] The second reaction is the tandem Friedel−Crafts alkylation/enantioselective protonation reaction (FC/EP reaction, Figure 1d). It also involves the conjugate addition of indoles to enones, but in this case the substrate carries a methyl group at the α position and no substituent at the β position. Hence, the chirality is introduced not in the conjugate addition step, but in the subsequent protonation step. This reaction represents an enantioselective protonation in water, which is a highly challenging reaction.[30] These two reactions are mechanistically similar, but the chiral center is created in different elementary reaction steps.[24]

https://dx.doi.org/10.1021/acscatal.0c01619
ACS Catal. 2020, 10, 11783−11790

Table 1. Results of the Tandem Friedel-Crafts/Enantioselective Protonation (FC/EP Reaction) of Indoles with 4[a]

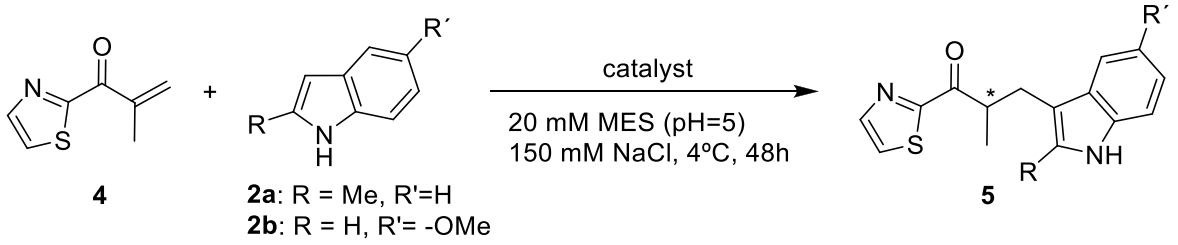

entry	indole	product	catalyst (μM)	yield of 5 (%)	*ee* (%)[b]
1	2b	5b	$Cu(NO_3)_2$	<5	
2	2b	5b	Cu(II)-phen	<5	
3	2b	5b	LmrR	10 ± 1	61 ± 2
4	2b	5b	$Cu(NO_3)_2$ + LmrR	86 ± 10	<5
5	2b	5b	Cu(II)-phen + LmrR	58 ± 12	−40 ± 2
6	2a	5a	Cu(II)-phen + LmrR	87 ± 14	59 ± 3

[a]Typical reaction conditions: **4** (1 mM), **2a**/**b** (1 mM) in 20 mM MES buffer (pH 5.0), 150 mM NaCl, at 4 °C for 72h; results are the average of at least two independent experiments, both carried out in duplicate. Error margins represent standard deviations. [b]determined by hplc; + and−signs indicate which is the major enantiomer peak based on order of elution, first and second, respectively.

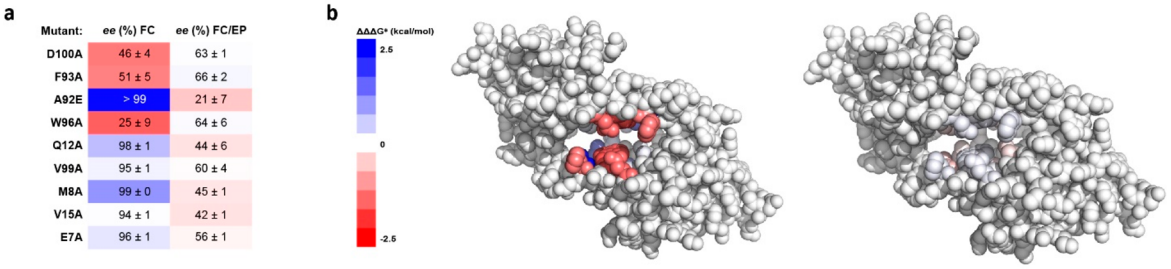

Figure 2. (a) Effect of mutations in LmrR on the *ee* of the catalyzed FC reaction between **1** and **2a** and FC/EP reaction between **4** and **2a**. Colors represent the difference between the $\Delta\Delta G^{\ddagger}$ values calculated from the corresponding *ee*'s as defined in panel b; (b) visualization of the mutated residues, and the effects on enantioselectivity, onto the crystal structure of LmrR/Cu(II)-phen (metal complex omitted for clarity). The effect of the mutation on the *ee*, compared to the wild-type LmrR, is visualized as a heatmap where the colors represent the difference between the $\Delta\Delta G^{\ddagger}$ values calculated from the corresponding *ee*'s ($\Delta\Delta\Delta G^{\ddagger} = \Delta\Delta G^{\ddagger}_{mutant} - \Delta\Delta G^{\ddagger}_{wildtype}$), indicating an increase (blue) or decrease (red) of enantioselectivity of the reaction catalyzed by the mutant compared to the wild type LmrR.

The conjugate addition of 5-methoxy-1H-indole (**2b**) to 2-methyl-1-(thiazol-2-yl)prop-2-en-1-one (**4**) was used as benchmark FC/EP reaction (Figure 1d, Table 1). The artificial metalloenzyme was prepared in situ by self-assembly from 9 mol % of $[Cu(phen)(NO_3)_2]$ with a slight excess (1.3 equiv) of LmrR in MES buffer at pH 5.0. Under these conditions, the product was obtained in 58% yield and 40% ee (entry 5). Reducing the amount of protein to 0.67 equiv, that is, using an excess of Cu(II)-phen, gave rise to a similar yield and ee (Table S5, entry 2 and 4). In absence of catalyst or when using Cu(II)-phen alone, without protein, almost no reaction was observed (entry 1 and 2). Interestingly, using LmrR alone, without Cu(II), gave rise to 10% yield of product with a significant ee of 61%, albeit of the opposite enantiomer compared to the artificial metalloenzyme (entry 3). As similar activity in this reaction was reported recently for the regulatory protein QacR.[31] Using a combination of $Cu(NO_3)_2$ with LmrR gave good activity, but no *ee* (entry 4), illustrating the importance of the phenanthroline ligand in recruiting the Cu(II) center to the protein. Combined these results show that, even though protein itself has some activity in this reaction, it is the combination of a Cu(II)-phen complex and LmrR that is responsible for achieving good catalytic activity and enantioselectivity. Evaluation of the indole scope showed that the best results were obtained using 2-methyl-1H-indole (**2a**), with 87% yield and 59% *ee* (entry 6) of product **5a**.

Mutagenesis Studies. Mutagenesis of residues at various positions in the hydrophobic pocket in spatial proximity to W96 was performed to establish where catalysis of both these reactions occur and which residues are important for activity. This included positions at the front entrance, i.e., D100, F93, and A92, residues in the pocket interior, i.e., M8, Q12, and V99 and residues V15, E7, which are placed in the back entrance of the pocket. Most of these residues were probed by converting them to alanine (alanine scanning), except at position A92 were alanine was already present. In this case mutation to glutamate, A92E was performed.

All mutants were evaluated in both the FC reaction of 2-methyl-indole (**2a**) with (*E*)-1-(1-methyl-1*H*-imidazol-2-yl)-but-2-en-1-one (**1**) and the tandem FC/EP reaction of **2a** with 2-methyl-1-(thiazol-2-yl)prop-2-en-1-one (**4**).

In the FC reaction significant effects on catalysis were observed in case of the front entrance mutants and the mutant M8A, which is located inside the pore (Figure 2 and Table S6). These results confirm that the reaction occurs in the pore, at the front entrance, close to the tryptophan residues where the Cu(II)-phen complex is bound. In most cases, the effect of the mutation was negative on both activity and enantioselectivity.

https://dx.doi.org/10.1021/acscatal.0c01619
ACS Catal. 2020, 10, 11783−11790

Two mutations gave rise to significantly improved enantioselectivity: the mutation M8A resulted in a strong increase in the *ee* to 99% (Table S6, entry 11) and A92E gave rise to both complete enantioselectivity (>99% *ee*) and a significantly increased product yield (Table S6, entry 6). As reported before, the W96A mutation caused a significant decrease in both yield and *ee* (Table S6, entry 2)

In contrast, almost all of these mutations had only a small effect on the results of the FC/EP reaction (Figure 2, Table S7). The W96A mutation caused a decrease in the yield, but surprisingly the ee remained similar or was even slightly higher (Table S7, entry 3). The only mutations that gave rise to a significant, negative, effect proved to be Q12E (Table S7, entry 10) and A92E (Table S7, entry 7). For the latter a decrease of the *ee* to 21% was obtained, which was unexpected since this same mutation proved to be the most beneficial for the FC reaction (vide supra). Reducing the amount of protein while keeping the Cu(II)-phen concentration the same caused a small increase of the ee to 32% (Table S5, entry 6).

Effect of Inhibitors. The role of the hydrophobic pocket in catalysis was probed by inhibition studies using Hoechst H33342, which has been shown to bind with nanomolar affinity in the pocket, sandwiched between W96 and W96′, analogous to binding of Cu(II)-phen as observed by X-ray crystallography.[25]

Fluorescence titration experiments show that H33342 can indeed displace the Cu(II)-phen from the pore of LmrR, albeit that more than 1 equiv is needed (SI, section V). Interestingly, in the presence of both Cu(II)-Phen and substrate **1** or **4**, resulting in the formation of the substrate bound complexes Cu(II)-phen -**1** and Cu(II)-phen-**4**, more equivalents of the Hoechst dye are required. This shows that both the substrate **1** and substrate **4** bound Cu(II) complexes do bind in the pocket and that this binding is stronger than that of Cu(II)-phen alone (SI, section V). These experiments show that H33342 may act as an inhibitor for catalysis, by displacing Cu(II)-phen or Cu(II)-phen-substrate complexes from their binding site. In view of the fact that both reactions are protein accelerated, this should have an effect on the results of catalysis. Indeed, addition of increasing amounts of H33342 up to 4 equiv with respect to Cu(II)-phen caused a significant decrease in the enantioselectivity in the FC reaction, to 57% *ee* (Table 2, entry 2). In case of the FC/EP reaction, after 16 h a lower yield was observed in the presence of 4 eq of H33342 compared to without, as expected. However, the *ee* was found to be higher in the presence of H33342 (Table 2, entries 3 and 4). After 72 h, the *ee* of the reaction in the presence of inhibitor decreased somewhat, which could suggest that H33342 causes racemization, albeit very slowly (Table 2).

Competition Experiments. Next, competition experiments were performed with the substrates **1** and **4**, using wild type LmrR and the mutants LmrR_W96A and LmrR_A92E (Figures 3 and S10). When 2-methylindole (**2a**) was combined with equimolar amounts of **1** and **4**, the corresponding products **3a** and **5a** were obtained in 66% and 17% yield, respectively, in the reaction catalyzed by LmrR/Cu(II)-phen, which corresponds to a selectivity of 80% for the FC reaction. The enantioselectivity of the products was similar to that obtained in the independent experiments. Notably, when we carried out these competition experiments with the LmrR variant A92E, the selectivity for the FC reaction increased to 96%; product **3a** was obtained in 66% yield and 98% *ee*, while only trace amounts of nearly racemic product **5a** were obtained. In contrast, when we used the mutant LmrR_W96A, the FC/EP reaction became the dominant activity, with a selectivity of 76%; product **5a** was obtained with 22% yield and 69% *ee*. These results show how with one single mutation, either one of these catalyzed reactions can be made the dominant activity of the artificial metalloenzyme.

Table 2. Results of the Competitive Binding of Hoechst 33342 to LmrR in the Friedel-Crafts (FC Reaction) and the Tandem Friedel-Crafts/Enantioselective Protonation (FC/EP Reaction)[a]

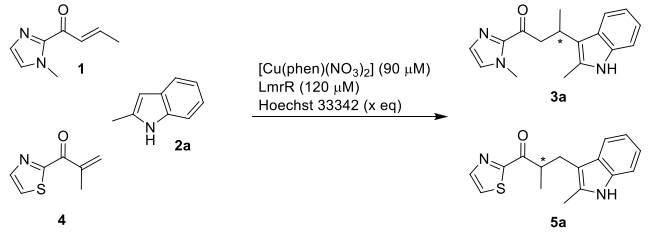

entry	substrate	Hoechst 33342 (eq)	time (h)	product	yield (%)	*ee* (%)
1	1	0	72	3a	41 ± 12	92 ± 2
2	1	4	72	3a	29 ± 18	57 ± 5
3[b]	4	0	16	5a	53 ± 6	56 ± 1
4[b]	4	4	16	5a	38 ± 1	73 ± 1
5[b]	4	0	72	5a	70 ± 16	58 ± 2
6[b]	4	4	72	5a	60 ± 6	61 ± 1

[a]Typical reaction conditions: **1**/**4** (1 mM), **2a** (1 mM), [Cu(II)-phen] (9 mol %; 90 μM), LmrR (12 mol %; 120 μM), H33342 (0 or 4 equiv with respect to the concentration of Cu(II)-phen) in 20 mM MOPS buffer (pH 7.0), 150 mM NaCl, at 4 °C; results are the average of at least two independent experiments, both carried out in duplicate. [b]20 mM MES buffer (pH 5.0), 150 mM NaCl.

Effect of A92 Mutation. While the effect of the W96A mutation is clear, that is, it eliminates a crucial part of the Cu(II)-phen binding site, the role of the glutamate residue in the A92E mutant was less obvious. The binding affinity of the [Cu(phen)$(NO_3)_2$] was determined (SI, Section VIII) and a dissociation constant (K_d) of 65 ± 19 nM and 59 ± 16 nM was found at pH 7 and 5, respectively. This represents a 2 orders of magnitude increase in binding affinity compared to WT LmrR (Table S9). Our initial hypothesis was that the carboxylate moieties would contribute to binding of the copper complex by interaction with the Cu(II) ion. For this reason, the corresponding glutamine mutant (i.e., A92Q) was prepared, since glutamine is sterically similar to glutamate, but is not a good ligand for Cu(II). However, the A92Q mutant also showed an increased affinity for Cu(II)-phen (K_d 103 ± 41 nM; Figure S12), albeit that the results in catalysis were similar to the wild-type LmrR (Tables S6, entry 7 and S7, entry 8). The increased affinity of the A92E mutant for Cu(II)-phen also allowed to determine the apparent catalytic efficiency of this improved mutant for the FC reaction: k_{cat}/K_M = 73.3 M^{-1} min^{-1} (Figure S14). This information could not be obtained for the wild type LmrR-based artificial metalloenzyme since, in this case, the binding affinity of the Cu(II)-phen complex to the wild type protein is moderate. At higher concentrations this causes the substrates to start displacing the Cu(II)-phen complex, which leads to a significant decrease of the catalytic activity.[28] Unfortunately, due to substrate solubility issues, the individual Michaelis Menten parameters k_{cat} and K_M could not be determined.

https://dx.doi.org/10.1021/acscatal.0c01619
ACS Catal. 2020, 10, 11783−11790

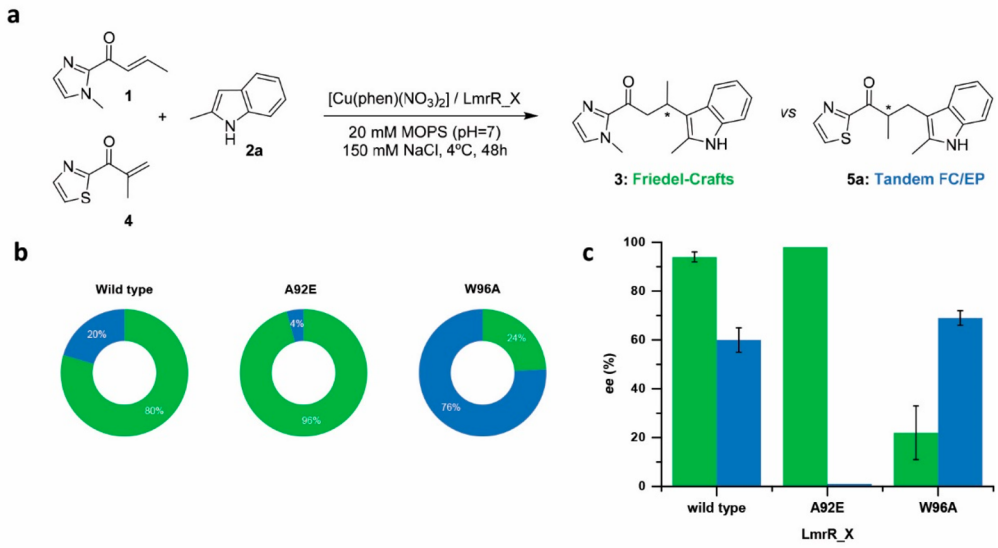

Figure 3. (a) Competition experiment between FC reaction of **1** with **2a** (and FC/EP reaction of **4** with **2a**) catalyzed by LmrR/Cu(II)-phen, LmrR_A92E/Cu(II)-phen and LmrR_W96A/Cu(II)-phen. All substrates were present in equimolar amounts (1 mM). (b) Relative product distribution (%) of the competing FC (green) and FC/EP reactions (blue). (c) *ee* values for products of the FC and FC/EP reaction in the competition experiment catalyzed by LmrR mutants with standard deviations shown.

Computation was then used to gain a better understanding about the effect of mutation A92E. For this purpose, the bis aqua form of the copper bound phenanthroline cofactor $[Cu(phen)(H_2O)_2]^{2+}$ was optimized via quantum calculations and embedded into the WT, A92E and A92Q variants of LmrR via protein−ligand docking (see details in the Supporting Information, section X). The best scored structures showed in all cases the copper-phenanthroline moiety at the center of the cavity packed between tryptophans W96/W96′, a result consistent with the X-ray structure. Those were subsequently submitted to 300 ns MD simulation.

The MD simulations for WT LmrR showed that hydrophobic interactions between A92 and V15 contribute to a somewhat closed arrangement of the active site, in which the indole rings of W96/W96′ are slightly tilted with respect to each other, in agreement with the X-ray structure (Figure 4, left). Hence, the π-stacking interactions between the indole rings of residues W96/W96′ and the phenanthroline ligand are not optimal. Hydrogen bonding interactions between the water ligands and residues D100/D100′ contribute to maintain the positioning of the copper cofactor.

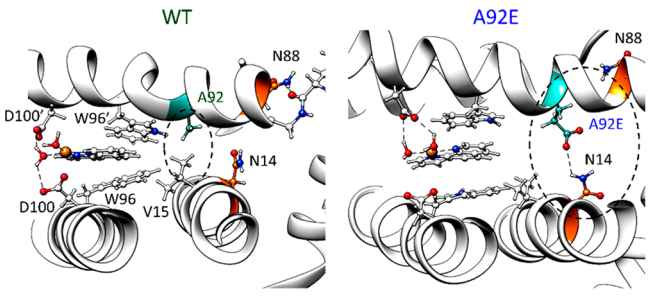

Figure 4. Comparison between representative structures of the pore along 300 ns of MD simulation for WT (left) and A92E (right) variants of LmrR with Cu(II)-phen bound. For WT, hydrophobic interactions between A92 and V15 promote closing of the active site, resulting in a not optimal π-stacking between both W96/W96′ and the phenanthroline ligand of the Cu(II)-phen cofactor. In contrast, the A92E mutant enables polar interactions with N14, which contribute to the opening of the active site and a parallel orientation of the W96/W96′ residues and, thus, cause a better binding of the phenanthroline ligand via π-stacking.

Instead, according to the MD simulations, the mutation of the alanine to glutamate in the A92E mutant disrupts the hydrophobic interaction and generates a hydrogen bonding network at the back of the active site, involving mainly residues N88 of helix α4 and N14, located at the opposite side of the cavity in helix α1 (Figures S16 and S17, left). This contributes to a different structural arrangement of the pore, with a parallel orientation of the W96/W96′ indoles and an expanded hydrophobic free volume of the cavity (Figures S18 and S19). The result is a better packing of the Cu(II)-phen complex by a dual π-stacking interaction from W96/W96′. Tentatively, this is related to the increased binding affinity, and causes the Cu(II)-phen being positioned deeper inside the pore (Figure S19). While these structures are found frequently in the A92E mutant (40% of the MD simulation), they are virtually nonexistent in case of the WT protein (1% of the MD simulation). Similar structures were observed for the A92Q mutant, albeit these were less frequent than for the A92E mutant (Supporting Information). These results suggest that the A92E mutation does not have a direct effect on catalysis, but mainly has a structural effect, which translates into stronger binding of the Cu(II)-phen complex.

DISCUSSION

The both reactions investigated here, the Cu(II)-phen/LmrR catalyzed FC and FC/EP reaction, are mechanistically similar, the only difference being that in the FC reaction the stereocenter is introduced in the conjugate addition step, whereas in the FC/EP reaction the stereocenter is created in the subsequent protonation of the enolate intermediate. Yet some marked differences were observed in how these reactions respond to mutations, addition of inhibitors and in competition experiments.

https://dx.doi.org/10.1021/acscatal.0c01619
ACS Catal. 2020, 10, 11783−11790

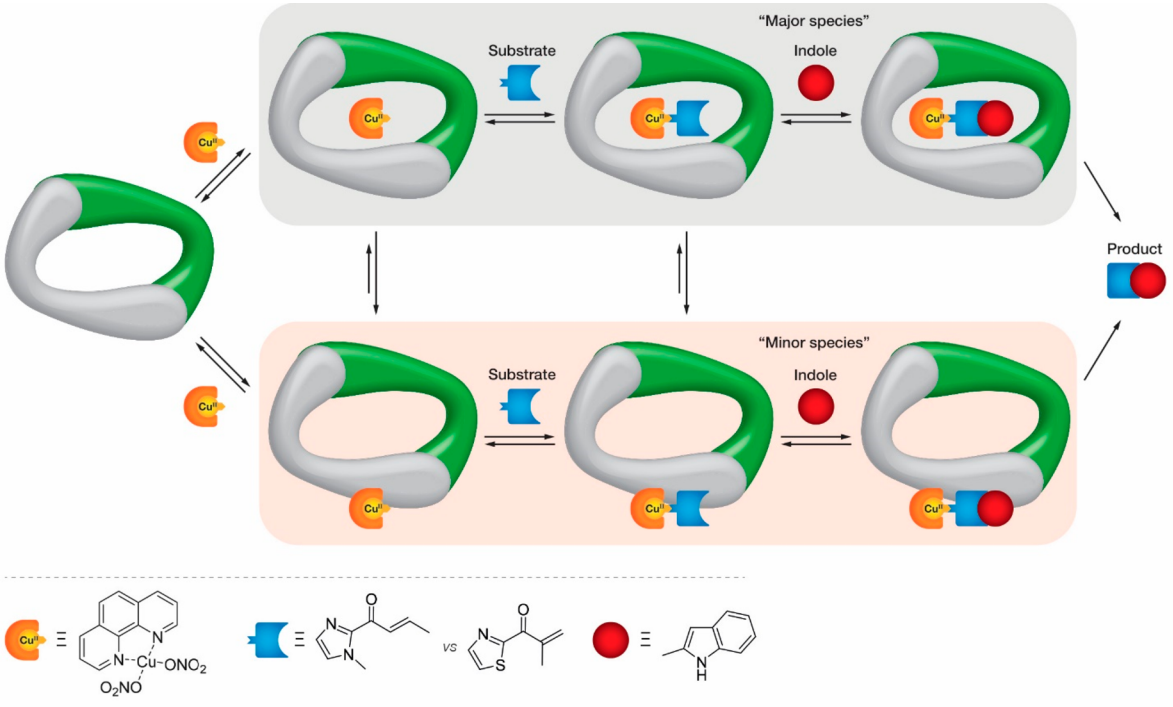

Figure 5. Schematic explanation of the observed metal cofactor binding dynamics of LmrR-based artificial metalloenzymes and the relation to catalysis. Most of the Cu(II)-phen complex will bind in the cavity between the two Trp residues W96/W96′ (primary active site), where it can bind and activate the substrate to undergo conjugate addition by an indole nucleophile, resulting in formation of the product (top pathway, "major species"). This pathway gives rise to the highest *ee*'s in the FC reaction. However, a small but non-neglible fraction of the Cu(II)-phen can bind at other positions in LmrR (secondary active sites) where it can also activate a substrate for reaction with the indole (lower pathway, "minor" species). This is the pathway that gives the highest ee in the FC/EP reaction. Note that the position of the metal cofactor in the protein in the lower pathway is arbitrary. At present, this secondary site/sites have not been identified.

The combined data suggest that the FC and FC/EP reaction both primarily occur in the hydrophobic pocket of LmrR, with the Cu(II)-phen catalytic complex bound between the two central tryptophans W96 and W96′ as suggested by the combined spectroscopy and X-ray crystallography data. This is supported by the fact that removing the tryptophans by mutation to alanine, or displacing the Cu(II)-phen from the pocket by addition of Hoechst H33342 as inhibitor results in a decrease of the yield of product in both reactions. Moreover, the mutagenesis study clearly shows that the ee's of the FC reaction are most affected by mutations in the center of the pore at the front entrance, near W96/W96′, where the Cu(II) site is located in the X-ray structure. Notable in this regard is the A92E mutation, which significantly increases the binding affinity of Cu(II)-Phen: this gives rise to the highest activity and selectivity in the FC reaction. In the case of the FC/EP reaction, the *ee*'s do not show strong dependence on most of the mutations in this location, but it should be noted that the stereocenter is created in a different elementary step and hence, may not be influenced by mutations in the same way.

However, some of the observations made for the FC/EP reaction appear to conflict with the active site being located at the front entrance of the pore and comprised of the Cu(II)-phen bound between the W96/W96'. For example, when this active site cannot form because Cu(II)-phen binding between the two tryptophans is blocked, by addition of the inhibitor Hoechst H33342, or by removal of W96/W96' by mutagenesis, the enantioselectivity of the reaction actually increases. Conversely, in cases where the binding of Cu(II)-phen is favored, such as in the A92E mutant, the enantioselectivity strongly decreases.

We propose that this apparent dichotomy can be resolved by considering the dynamics of binding of the Cu-phen cofactor, which is a result of the moderate binding affinity of Cu(II)-phen for wild type LmrR. This means that under the conditions of catalysis, most of the Cu(II)-phen is bound between the tryptophans, which is the primary active site. However, a non-neglible fraction of the Cu(II) complex does not bind there and, most likely, can interact at another position of the protein. At present, the location of this secondary active site is unknown. It also cannot be ruled out that there is more than one secondary site. These secondary active sites could be at a different position in or close to the hydrophobic pore but could also be on the surface of the protein (Figure 5). The role of the protein is clear as the FC/EP reaction does not occur, or only very slowly, in the absence of protein combined with the enantioselectivity of product **5**. This means that the ARM is not one well-defined species, but a mixture of copper complexes residing in a different protein microenvironment and the outcome of the catalysis is the weighted average of the contribution of these different active sites. This is highly reminiscent of what was observed before in our work on salmon testes DNA-based catalysis.[23]

In both the FC and FC/EP reaction, the primary active site dominates the outcome of catalysis because most of the Cu(II)-phen and the intermediates [Cu(II)-phen-**1**] and [Cu(II)-phen-**2**] are bound here and it significantly accelerates the reaction. This is also the reason that, when using an excess of Cu(II)-phen compared to protein, the results of catalysis do

https://dx.doi.org/10.1021/acscatal.0c01619
ACS Catal. 2020, 10, 11783−11790

not decrease. In case of the FC reaction this also gives the highest enantioselectivity. But in case of the FC/EP reaction, it appears that the primary site is not the most enantioselective, but the secondary site(s). Indeed by blocking or eliminating the primary active site by removal of W96, the relative contribution of secondary site(s) increases, resulting in a higher *ee*. Conversely, by favoring the primary active site through the A92E mutation, which strongly increases the affinity of Cu(II)-phen for binding between W96/W96′, basically there is/are no more secondary site(s), resulting in a decreased enantioselectivity in the FC/EP reaction but an increase in the FC reaction. By using an excess of Cu(II)-phen compared to LmrR_A92E mutant, some of the secondary sites get occupied again, which is reflected in an small increase of *ee* in the case of the FC/EP reaction.

The competition experiments are in agreement with this hypothesis. Using LmrR, both the FC and FC/EP reaction are possible, but the former is preferred in the primary active site. Making a single mutation, A92E, results in further favoring of reaction via the primary active site (top pathway) and the secondary site(s) (lower pathway) is effectively shut down (Figure 5). This is reflected in the results: the A92E mutant strongly prefers the FC reaction over the FC/EP reaction. Conversely, by removing the central tryptophans via the W96A mutation only the lower pathway can be followed, since it eliminates the preferred primary binding site for the Cu(II)-phen complex. The FC reaction is still possible, albeit with lower activity and selectivity. In this case, the FC/EP reaction is now the favored reaction, resulting in an increased yield and enantioselectivity of the FC/EP product.

CONCLUSION

In conclusion, the LmrR/Cu(II)-phen artificial metalloenzyme shows dynamic behavior in the positioning of its abiological metal cofactor, which, in turn, is related to the activity and selectivity in catalysis. In the WT LmrR/Cu(II)-phen, the FC reaction, which occurs in the primary active site in the hydrophopbic pore of the protein, is the preferred activity. However, it exhibits lower, but significant, levels of activity for another reaction, the FC/EP reaction, which is mechanistically similar but involves an enantioselective protonation step. However, the FC/EP reaction achieves the highest enantioselectivity when it occurs in a secondary active site. By only one mutation, A92E, this artificial metalloenzyme became almost fully selective for the FC reaction, while by another mutation, i.e., W96A, the FC/EP reaction became the dominant activity. The switching of preferred activity and selectivity by dynamic interconversion of the position of a metal cofactor has not been described for natural enzymes and, to date, appears to be particular for artificial metalloenzymes. Thus, this study underlines the importance of cofactor binding dynamics as a key element of artificial enzyme design.

ASSOCIATED CONTENT

Supporting Information

The Supporting Information is available free of charge at https://pubs.acs.org/doi/10.1021/acscatal.0c01619.

Detailed experimental procedures, characterization data for all new compounds and proteins, additional catalysis and biophysical data, X-ray crystallography data, details for molecular dynamics (MD) simulations, and DFT calculations (PDF)

AUTHOR INFORMATION

Corresponding Authors

Lara Villarino − *Stratingh Institute for Chemistry, University of Groningen, 9747, AG, Groningen, The Netherlands;* orcid.org/0000-0003-4728-2001; Email: lara.villarino@usc.es

Gerard Roelfes − *Stratingh Institute for Chemistry, University of Groningen, 9747, AG, Groningen, The Netherlands;* orcid.org/0000-0002-0364-9564; Email: j.g.roelfes@rug.nl

Authors

Shreyans Chordia − *Stratingh Institute for Chemistry, University of Groningen, 9747, AG, Groningen, The Netherlands*

Lur Alonso-Cotchico − *Stratingh Institute for Chemistry, University of Groningen, 9747, AG, Groningen, The Netherlands;* orcid.org/0000-0002-0172-6394

Eswar Reddem − *Stratingh Institute for Chemistry, University of Groningen, 9747, AG, Groningen, The Netherlands*

Zhi Zhou − *Stratingh Institute for Chemistry, University of Groningen, 9747, AG, Groningen, The Netherlands;* orcid.org/0000-0001-7926-118X

Andy Mark W. H. Thunnissen − *Groningen Biomolecular Sciences and Biotechnology Institute, University of Groningen, 9747, AG, Groningen, The Netherlands*

Jean-Didier Maréchal − *Departament de Química, Universitat Autònoma de Barcelona, 08193 Barcelona, Spain;* orcid.org/0000-0002-8344-9043

Complete contact information is available at: https://pubs.acs.org/10.1021/acscatal.0c01619

Notes

The authors declare no competing financial interest.

ACKNOWLEDGMENTS

We acknowledge the European Synchrotron Radiation Facility for provision of synchrotron radiation facilities. The authors thank R. Leveson-Gower for assistance in catalysis experiments. This project was supported by the European Research Council (ERC starting Grant No. 280010), The Netherlands Organisation for Scientific Research (NWO; Vici Grant 724.013.003), a postdoctoral grant from Xunta de Galicia (Plan I2C, to L.V.), and a grant from the Spanish MINECO (CTQ2017-87889-P). G.R. acknowledges support from the Ministry of Education Culture and Science (Gravitation Programme No. 024.001.035).

REFERENCES

(1) Schwizer, F.; Okamoto, Y.; Heinisch, T.; Gu, Y.; Pellizzoni, M. M.; Lebrun, V.; Reuter, R.; Köhler, V.; Lewis, J. C.; Ward, T. R. Artificial Metalloenzymes: Reaction Scope and Optimization Strategies. *Chem. Rev.* **2018**, *118*, 142−231.

(2) Davis, H. J.; Ward, T. R. Artificial Metalloenzymes: Challenges and Opportunities. *ACS Cent. Sci.* **2019**, *5*, 1120−1136.

(3) Drienovská, I.; Roelfes, G. Artificial Metalloenzymes for Asymmetric Catalysis by Creation of Novel Active Sites in Protein and DNA Scaffolds. *Isr. J. Chem.* **2015**, *55*, 21−31.

(4) Pàmies, O.; Diéguez, M.; Bäckvall, J.-E. Artificial Metalloenzymes in Asymmetric Catalysis: Key Developments and Future Directions. *Adv. Synth. Catal.* **2015**, *357*, 1567−1586.

(5) Lewis, J. C. Artificial Metalloenzymes and Metallopeptide Catalysts for Organic Synthesis. *ACS Catal.* **2013**, *3*, 2954−2975.

(6) Natoli, S. N.; Hartwig, J. F. Noble-Metal Substitution in Hemoproteins: An Emerging Strategy for Abiological Catalysis. *Acc. Chem. Res.* **2019**, *52*, 326−335.
(7) Oohora, K.; Onoda, A.; Hayashi, T. Hemoproteins Reconstituted with Artificial Metal Complexes as Biohybrid Catalysts. *Acc. Chem. Res.* **2019**, *52*, 945−954.
(8) Pauling, L. Nature of Forces between Large Molecules of Biological Interest. *Nature* **1948**, *161*, 707−709.
(9) James, L. C.; Tawfik, D. S. Conformational Diversity and Protein Evolution - A 60-Year-Old Hypothesis Revisited. *Trends Biochem. Sci.* **2003**, *28*, 361−368.
(10) Tokuriki, N.; Tawfik, D. S. Protein Dynamism and Evolvability. *Science* **2009**, *324*, 203−207.
(11) Hammes-Schiffer, S. Catalytic Efficiency of Enzymes: A Theoretical Analysis. *Biochemistry* **2013**, *52*, 2012−2020.
(12) Petrović, D.; Risso, V. A.; Kamerlin, S. C. L.; Sanchez-Ruiz, J. M. Conformational Dynamics and Enzyme Evolution. *J. R. Soc., Interface* **2018**, *15*, 20180330.
(13) Leveson-Gower, R. B.; Mayer, C.; Roelfes, G. The Importance of Catalytic Promiscuity for Enzyme Design and Evolution. *Nature Rev. Chem.* **2019**, *3*, 687−705.
(14) Huang, X.; Garcia-Borràs, M.; Miao, K.; Kan, S. B. J.; Zutshi, A.; Houk, K. N.; Arnold, F. H. A Biocatalytic Platform for Synthesis of Chiral α-Trifluoromethylated Organoborons. *ACS Cent. Sci.* **2019**, *5*, 270−276.
(15) Villarino, L.; Splan, K. E.; Reddem, E.; Alonso-Cotchico, L.; Gutiérrez de Souza, C.; Lledós, A.; Maréchal, J.-D.; Thunnissen, A.-M. W. H.; Roelfes, G. An Artificial Heme Enzyme for Cyclopropanation Reactions. *Angew. Chem., Int. Ed.* **2018**, *57*, 7785−7789.
(16) Markel, U.; Sauer, D. F.; Schiffels, J.; Okuda, J.; Schwaneberg, U. Towards the Evolution of Artificial Metalloenzymes-A Protein Engineer's Perspective. *Angew. Chem., Int. Ed.* **2019**, *58*, 4454−4464.
(17) Hyster, T. K.; Ward, T. R. Genetic Optimization of Metalloenzymes: Enhancing Enzymes for Non-Natural Reactions. *Angew. Chem., Int. Ed.* **2016**, *55*, 7344−7357.
(18) Yang, H.; Swartz, A. M.; Park, H. J.; Srivastava, P.; Ellis-Guardiola, K.; Upp, D. M.; Lee, G.; Belsare, K.; Gu, Y.; Zhang, C.; Moellering, R. E.; Lewis, J. C. Evolving Artificial Metalloenzymes via Random Mutagenesis. *Nat. Chem.* **2018**, *10*, 318−324.
(19) Jing, Q.; Okrasa, K.; Kazlauskas, R. J. Stereoselective Hydrogenation of Olefins Using Rhodium-Substituted Carbonic Anhydrase-A New Reductase. *Chem. - Eur. J.* **2009**, *15*, 1370−1376.
(20) Jing, Q.; Kazlauskas, R. J. Regioselective Hydroformylation of Styrene Using Rhodium-Substituted Carbonic Anhydrase. *ChemCatChem* **2010**, *2*, 953−957.
(21) Key, H. M.; Clark, D. S.; Hartwig, J. F. Generation, Characterization, and Tunable Reactivity of Organometallic Fragments Bound to a Protein Ligand. *J. Am. Chem. Soc.* **2015**, *137*, 8261−8268.
(22) Boersma, A. J.; Megens, R. P.; Feringa, B. L.; Roelfes, G. DNA-Based Asymmetric Catalysis. *Chem. Soc. Rev.* **2010**, *39*, 2083−2092.
(23) Boersma, A. J.; Klijn, J. E.; Feringa, B. L.; Roelfes, G. DNA-Based Asymmetric Catalysis: Sequence-Dependent Rate Acceleration and Enantioselectivity. *J. Am. Chem. Soc.* **2008**, *130*, 11783−11790.
(24) García-Fernández, A.; Megens, R. P.; Villarino, L.; Roelfes, G. DNA-Accelerated Copper Catalysis of Friedel-Crafts Conjugate Addition/Enantioselective Protonation Reactions in Water. *J. Am. Chem. Soc.* **2016**, *138*, 16308−16314.
(25) Madoori, P. K.; Agustiandari, H.; Driessen, A. J. M.; Thunnissen, A.-M. W. H. Structure of the Transcriptional Regulator LmrR and Its Mechanism of Multidrug Recognition. *EMBO J.* **2009**, *28*, 156−166.
(26) Takeuchi, K.; Tokunaga, Y.; Imai, M.; Takahashi, H.; Shimada, I. Dynamic Multidrug Recognition by Multidrug Transcriptional Repressor LmrR. *Sci. Rep.* **2015**, *4*, 6922.
(27) van der Berg, J. P.; Madoori, P. K.; Komarudin, A. G.; Thunnissen, A.-M.; Driessen, A. J. M. Binding of the Lactococcal Drug Dependent Transcriptional Regulator LmrR to Its Ligands and Responsive Promoter Regions. *PLoS One* **2015**, *10*, e0135467.
(28) Bos, J.; Browne, W. R.; Driessen, A. J. M.; Roelfes, G. Supramolecular Assembly of Artificial Metalloenzymes Based on the Dimeric Protein LmrR as Promiscuous Scaffold. *J. Am. Chem. Soc.* **2015**, *137*, 9796−9799.
(29) Roelfes, G. LmrR: A Privileged Scaffold for Artificial Metalloenzymes. *Acc. Chem. Res.* **2019**, *52*, 545−556.
(30) Mohr, J. T.; Hong, A. Y.; Stoltz, B. M. Enantioselective Protonation. *Nat. Chem.* **2009**, *1*, 359−369.
(31) Gutiérrez de Souza, C.; Alonso-Cotchico, L.; Bersellini, M.; Roelfes, G. Unexpected Catalytic Activity of the Regulatory Protein QacR. 2020 DOI: 10.26434/chemrxiv.12662003.v1.

https://dx.doi.org/10.1021/acscatal.0c01619
ACS Catal. 2020, 10, 11783−11790